Unraveling Excited-State Dynamics in a Polyfluorene-Perylenediimide Copolymer

Eduard Fron,[†] Ania Deres,[†] Susana Rocha,[†] Gang Zhou,[‡] Klaus Müllen,[‡] Frans C. De Schryver,[†] Michel Sliwa,[§] Hiroshi Uji-i,[†] Johan Hofkens,[†] and Tom Vosch*,[†]

Department of Chemistry and Institute for Nanoscale Physics and Chemistry, Katholieke Universiteit Leuven, Celestijnenlaan 200F, 3001 Heverlee, Belgium, Max-Planck-Institut für Polymerforschung, Ackermannweg 10, 55128 Mainz, Germany, and Laboratoire de Spectrochimie Infrarouge et Raman (UMR 8516 du CNRS), Centre d'Etudes et de Recherches Lasers et Applications (FR 2416 du CNRS), Université Lille 1 Sciences et Technologies de Lille, Bât C5, 59655 Villeneuve d'Ascq Cedex, France

Received: September 29, 2009; Revised Manuscript Received: December 10, 2009

Insight into the exciton dynamics occurring in a polyfluorene-perylenediimide (**PF-PDI**) copolymer with a reaction mixture ratio of 100 fluorene units to 1 *N*,*N*′-bis(phenyl)-1,6,7,12-tetra(*p-tert*-octylphenoxy)-perylene-3,4,9,10-tetracarboxylic acid diimide (**PDI**) is presented here. Time-correlated single photon counting and femtosecond transient absorption spectroscopy measurements on the **PF-PDI** copolymer have been employed to investigate the excited-state properties of the polyfluorene subunit where the exciton is localized (**PF**) and the incorporated **PDI** chromophore. The experimental results were compared with those obtained from a polyfluorene polymer (**model PF**) and a *N*,*N*′-bis(2,6-diisopropylphenyl)-1,6,7,12-tetra(*p-tert*-octylphenoxy)-perylene-3,4,9,10-tetracarboxylic acid diimide (**model PDI**) which were used as reference compounds. Because of the high polydispersity of the **PF-PDI** copolymer, there is a polymer fraction present that contains no **PDI** chromophores (polyfluorene polymer fraction (**PF polymer fraction**)), and wide-field imaging of single polymers chains of the synthesized **PF-PDI** copolymer was used to estimate this **PF polymer fraction**. Following the primary excitation of the **PF** in the **PF-PDI** copolymer, energy hopping between **PF**'s can occur. A fraction of the energy of the absorbed photons will be transferred to a **PDI** chromophore via energy transfer from a **PF**. In a polar solvent, a charge transfer state having the S_1 of the **PDI** moiety as a precursor state is found to form with high efficiency on a nanosecond time scale. The data suggest that a fraction of the absorbed energy is directed, transferred, and used in charge separation, providing a clear view of a multistep mechanism of exciton dissociation into charges.

Introduction

The properties and dynamics of the excited states provide important information for the detailed understanding of complex processes often occurring in conjugated polymers. Investigation and tuning of these photophysical processes led to the development of new functional polymer materials for optoelectronic applications.[1,2] One approach of tuning the spectroscopic properties is by controlling the effective conjugation length.[3] Extending the conjugation length in a polymer chain leads to a bathochromic shift of the absorption and emission characteristics.[4] However, the presence of sites of different conjugation lengths can contribute to the formation of energy traps as the sites with the largest conjugation act as local minima. While application-tailored spectroscopic properties were achieved, the increased complexity of these multichromophoric systems involving either chromophore−chromophore interactions or intrinsic conformations motivates the study of specific systems containing well-known donor/acceptor units. However, the study of the excited-state dynamics of polymer chains with incorporated chromophores or donor/acceptor units remains a challenge, mainly for two reasons. First, the large polydispersity and the difficulty in controlling the ratio of the constituents per chain in the synthesis processes can result in a distribution of kinetic components in time-resolved ensemble experiments. Also, small fractions of impurities or uncoupled subunits can show up in the observations, which could lead to erroneous conclusions. Second, competing excited-state processes such as singlet exciton migration, triplet formation, or charge transfer are more likely to occur, possibly affecting the fluorescence emission and making, for example, single molecule investigations complex and challenging.[5−11]

Among the various types of conjugated systems, polyfluorene copolymers have shown remarkable luminescence and optoelectronic properties[12−15] that can be tuned toward the development of promising alternatives to inorganic light-emitting diodes (LEDs),[16,17] and polymer-based solar cells.[18−21] Attaching molecular moieties with energy-accepting and highly luminescent properties (rylene dyes, phenylene vinylene units, etc.)[15,22,23] to the polyfluorene π-system also offers the prospect of tuning the emission wavelength for polymer-based LED applications.[16] Polyfluorene-based polymers with fluorene segments and molecular units with electron accepting or donating properties were shown to improve the overlap with the solar spectrum in polymer-based solar cells.[24,25] Also, for instance, in a polyfluorene/fullerene blend, a high conversion efficiency of the excitation energy into charges has been observed at low acceptor concentration.[26] While the efficiency of light absorption is basically improved, the charge generation and recombination, which is a key factor in their performance, remains poorly investigated, and their understanding requires further assessment. Hence, it is important to study and understand conformational

* To whom correspondence should be addressed. E-mail: Tom.Vosch@chem.kuleuven.be.
[†] Katholieke Universiteit Leuven.
[‡] Max-Planck-Institut für Polymerforschung.
[§] Université Lille 1 Sciences et Technologies de Lille.

10.1021/jp909295h
Published on Web 01/05/2010

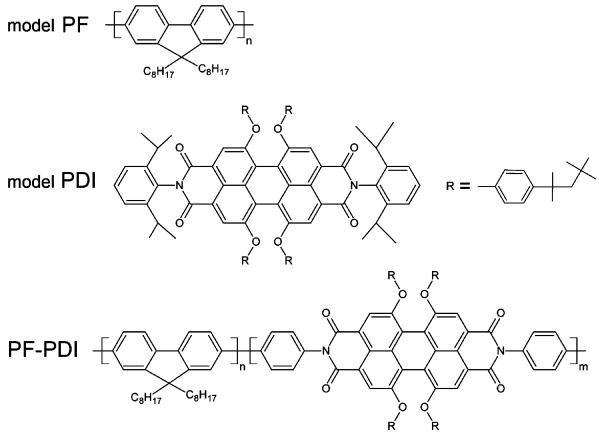

Figure 1. Chemical structures of **model PF**, **model PDI**, and **PF-PDI**. The reaction mixture ratio of *n* to *m* is 100 to 1.

aspects, the energy transfer pathways, exciton dynamics, and charge conversion in conjugated polymers and more specifically in polyfluorene systems. For example, the degree of planarity between the adjacent fluorene units was shown to substantially change the electronic and optical properties. By monitoring the energy of the 0−0 transition, Feldmann et al. classified single molecules belonging to three different phases, depending on the degree of planarization.[27] Besides local polymer conformations and the presence of chromophores with longer conjugation lengths (emissive traps), random chemical defects[28] could modify the exciton diffusion significantly, resulting in very different steady-state emission properties. Therefore, it is relevant to understand the energy transfer pathways, exciton dynamics, and charge conversion of the polyfluorene systems in different environments.

In this study, we explore the photophysical properties and dynamics of a polyfluorene-perylenediimide copolymer (**PF-PDI**) upon excitation of the **PF** (the polyfluorene subunit where the exciton is localized) and **PDI** (the *N*,*N*′-bis(phenyl)-1,6,7,12-tetra(p-tert-octylphenoxy)-perylene-3,4,9,10-tetracarboxylic acid diimide chromophore) parts by both ensemble and single-molecule techniques. The results of the ensemble measurements were then compared with those obtained from two reference compounds: a polyfluorene polymer (**model PF**) and *N*,*N*′-bis(2,6-diisopropylphenyl)-1,6,7,12-tetra(*p-tert*-octylphenoxy)-perylene-3,4,9,10-tetracarboxylic acid diimide (**model PDI**). Time-correlated single-photon counting (TC-SPC) and femtosecond transient absorption techniques were employed to unveil and identify the excited-state processes. We explore various aspects such as the localization of the primary exciton, its migration along the polymer chain, and the properties of the electronic excited states in solvents of different polarity. Because of the high polydispersity of the **PF-PDI** copolymer, there is a polymer fraction present that contains no **PDI** chromophores (polyfluorene polymer fraction (**PF polymer fraction**)). Wide-field imaging[29] of single polymers chains of the synthesized **PF-PDI** copolymer was used to estimate this **PF polymer fraction** in order to obtain a quantitative estimation of the energy transfer occurring in the **PF-PDI** copolymer fraction.

Experimental Section

Synthesis of Materials. The syntheses of **model PDI**, **model PF**, and **PF-PDI** were described previously,[16] and their chemical structures are shown in Figure 1. Briefly, for the synthesis of the **PF-PDI** copolymer, a mixture of *N*,*N*′-bis(4-bromophenyl)-1,6,7,12-tetra(*p-tert*-octylphenoxy)-perylene-3,4,9,10-tetracarboxylic acid diimide (1%) and 2,7-dibromo-9,9-dioctylfluorene was polymerized with nickel(0) in dimethylformamide (DMF)−toluene for 24 h, followed by a reaction with an excess of bromobenzene to remove any residual terminal bromine functionality (end-capping). The **PF-PDI** has an average molecular weight of about 130500 $g \cdot mol^{-1}$, a polydispersity index of 3.83 (see Ego et al. for further details),[16] and, based on the starting reaction mixture ratio, could contain on average of 1% of **PDI** units. The large polydispersity index together with M_n and the percentage of incorporated **PDI**'s result in a very broad chain length distribution of polymeric macromolecules as well as a broad distribution of the number of **PDI** units present in the individual chains (as a result of this, there is also a fraction containing no **PDI** units). Wide-field imaging of individual polymers chains was used to determine the size of the fraction of polymer chains that do not contain any **PDI** chromophores, the **PF polymer fraction** (vide infra). Before measuring the photophysical properties of the **PF-PDI** copolymer, an extra purification step was performed to remove nonincorporated **PDI**s (a fraction of 0.18 was removed; see Supporting Information). These free **PDI**s were removed by passing the **PF-PDI** copolymer through a recycling high-performance liquid chromatography/gel permeation chromatography (HPLC/GPC) system (LC-9101 from Japan Analytical Industry Co. Ltd.).

Steady State Measurements. The stationary measurements were recorded in cyclohexane (dielectric constant = 2, refractive index = 1.42), toluene (dielectric constant = 2.43, refractive index = 1.49), chloroform (dielectric constant = 4.8, refractive index = 1.44), tetrahydrofuran (THF, dielectric constant = 7.6, refractive index = 1.4) and benzonitrile (PhCN, dielectric constant = 25, refractive index = 1.52) as solvents of different polarity using a spectrophotometer (Lambda 40, Perkin-Elmer) and a fluorimeter (Fluorolog FL3−11, Perkin-Elmer) corrected for the wavelength dependence of the detection system.[30] All solvents were spectroscopic grade. The optical density at the absorption maximum of all solutions was kept below 0.1 in a 1 cm cuvette, and for the emission spectra the excitation wavelengths were set to 375 and 543 nm for the **PF** and **PDI** moieties, respectively. The fluorescence quantum yields of the compounds were determined using perylene in toluene (for λ_{ex} = 390 nm, $\Phi_f = 0.71$) and cresyl violet in ethanol (for λ_{ex} = 543 nm, $\Phi_f = 0.5$) as references.[31,32]

Single Molecule Wide-Field Imaging and Analysis. Wide-field imaging of single **PF-PDI** molecules was performed using an inverted optical microscope (IX71, Olympus) equipped with a 1.3 N.A., 100× oil immersion objective (Plan Fluorite, Olympus) and a highly sensitive cooled charge-coupled device (CCD) camera with 512 × 512 pixels (Hamamatsu EM-CCD ImagEM Model C9100−13) with a pixel size of 16 × 16 μm^2. For excitation, 532 nm light from a diode-pumped solid state laser (CDPS532M-50, JDS Uniphase Co.) and 375 nm light from a CW diode laser (Excelsior Diode CW Laser, Spectra-Physics) were used. Excitation intensities were set to 250W/cm^2 for 532 nm and 10W/cm^2 for 375 nm. The wide-field illumination for excitation was achieved by focusing the expanded and collimated laser beam onto the back-focal plane of the objective. The polarization of the excitation light in the sample plane was carefully tuned to be circular using zero-order $\lambda/4$ waveplates to compensate for polarization shifts of the dichroic mirror. Emission was collected by the same objective and imaged by the CCD after passing through a dichroic mirror (z532rdc, Chroma Technology Co.) and an additional spectral filter (HQ545LP or HQ400LP, Chroma Technology Co.), removing the excitation light. The image was further magnified

3.3 times with a camera lens (Olympus) before the CCD camera, resulting in a maximum field of view of 24.6 × 24.6 μm^2 (48 × 48 nm^2 per pixel). All measurements were done at room temperature under ambient atmosphere. The obtained images were analyzed using a routine written in MatLab software, in order to reconstruct the intensity trajectory of a single spot in the recorded movies (0.5 s integration time per frame).[33] Samples were prepared by spin-casting $\sim 10^{-10}$ M solutions of the **PF-PDI** copolymer dissolved in toluene containing 5 mg/mL poly(methyl methacrylate) polymer (PMMA, Aldrich, $M_w \approx$ 93 000) onto thoroughly cleaned glass coverslips.

Picosecond Fluorescence TC-SPC Experiments. The fluorescence decay times have been determined by TC-SPC measurements described in detail previously.[34] A time-correlated single photon timing PC module (SPC 830, Becker & Hickl) was used to obtain the fluorescence decay histogram in 4096 channels. The decays were recorded with 10 000 counts in the peak channel in time windows of 25 and 15 ns corresponding to 6 ps/ch and 3.7 ps/ch and analyzed globally with time-resolved fluorescence analysis (TRFA) software.[35,36] The full width at half-maximum (fwhm) of the instrument response function (IRF) was typically on the order of 40 ps. The quality of the fits has been judged by the fit parameters χ^2 (<1.2), Z_χ^2 (<3) and the Durbin−Watson parameter (1.8 < DW < 2.2) as well as by the visual inspection of the residuals and autocorrelation function.[37] All measurements were performed in toluene and THF in a 1 cm optical path length cuvette at an optical density of ca. 0.1 at the excitation wavelength of 375 and 543 nm for the **PF** and **PDI** units, respectively. As a control, experiments were also performed on degassed samples, which yielded the same decay components with similar amplitudes. For these experiments, samples were degassed using the consecutive freeze−pump−thaw cycle method.

Femtosecond Transient Absorption Measurements. The experiments were performed with an amplified femtosecond double optical parametric amplifier (OPA) laser system, which has been described previously,[38] providing an intense pulse used for excitation (395 nm) and a weak pulse used for probing the changes in absorption in a wavelength range between 470 and 770 nm. The probe light was generated by focusing an 800-nm beam in a 3 mm sapphire plate to obtain a white light continuum in the visible region. The monochromatic detection was performed using a PMT (R1527p, Hamamatsu) placed at the second exit of the spectrograph mounted behind a slit. The pulse duration was 250 fs (fwhm) at the sample position as determined by cross correlation. The probing was done under magic angle conditions (54.7° relative orientation between the pump and probe light polarization planes). The highest value in optical density change observed was still well below the saturation level (about 400 mOD).

The compounds were dissolved in toluene and THF at a concentration that yielded an absorbance of ca. 0.4 per mm. The sample was contained in a quartz cuvette with an optical path length of 1 mm. To improve the signal-to-noise ratio, every measurement was averaged 15 times at 512 delay positions where a delay position is referred to as the time interval between the arrival of the pump and the probe pulses at the sample position. After each experiment, the integrity of the samples was checked by recording the steady-state absorption and emission spectra and comparing them with those obtained before the experiments. No spectral changes suggesting photodegradation were observed.

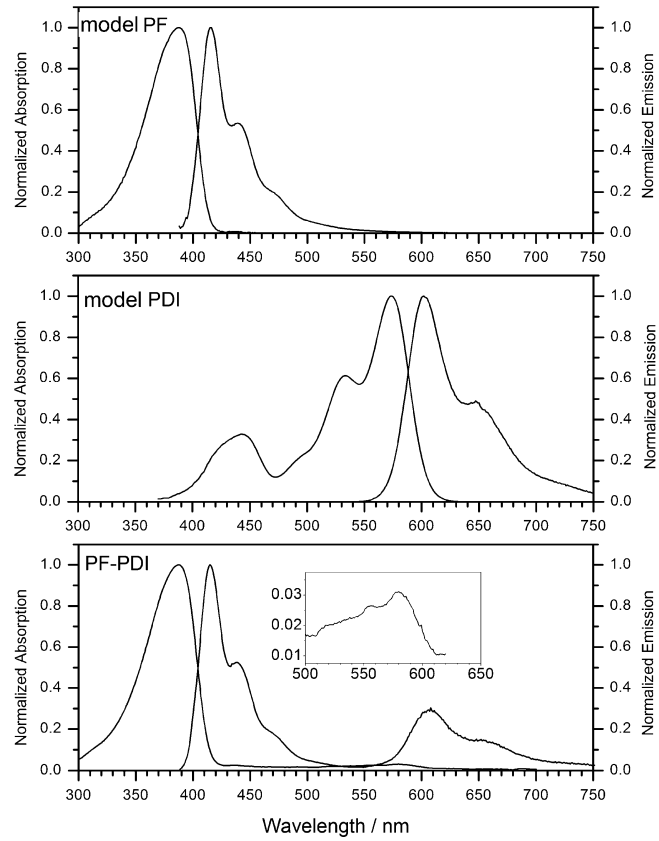

Figure 2. Normalized steady-state absorption and emission spectra of **model PF**, **model PDI**, and **PF-PDI** in toluene (λ_{ex} = 375 nm for **model PF** and **PF-PDI** and λ_{ex} = 543 nm for **model PDI** and **PF-PDI**). Inset: magnification of the absorption spectrum of **PF-PDI** in the 500−650 nm region.

Results and Discussion

Steady-State Measurements. The absorption and emission spectra of **model PF**, **model PDI**, and **PF-PDI** were recorded in five solvents of different polarity: Cyclohexane, toluene, THF, chloroform, and PhCN. The steady-state spectra in toluene are shown in Figure 2, whereas the absorption and emission maxima are presented in Table 1. The fluorescence quantum yields of the compounds were measured in toluene and THF, and the respective values are compiled in Table 2.

Model PF. The **model PF** compound has an intense absorption band peaking at 387 nm in toluene (394 nm in THF), which is attributed to the $\pi-\pi^*$ transition of the aromatic moieties of the fluorene units. Klaerner et al. have shown that, for polyfluorene derivatives, the absorption maximum could range from 348 (trimer) to 384 nm (decamer) in THF.[39] The 660 cm^{-1} (10 nm) red shift observed in the absorption of **model PF** in THF indicates that the conjugation length is about 12 fluorene units.[39−41] The **model PF** compound shows an emission with fluorescence maxima between 410 and 421 nm. A systematic red shift is observed in both absorption and emission maxima in solvents of increasing polarity. The compound has a quantum yield of 0.67 (0.60) in toluene (THF), which is consistent with the values reported in literature where values starting from 0.6 and up are reported.[42] The widespread of reported values could be related either to the number average molecular weight of the polymer or to the presence of chemical defects within the polymer backbone.[43,44,14,17]

Model PDI. The absorption spectrum of the **model PDI** system shows two bands that peak at 535 and 575 nm corresponding to the (0−0) and (0−1) vibronic features of the

TABLE 1: Absorption and Emission Maxima of Model PF, Model PDI and PF-PDI[a]

compound		cyclohexane		toluene		$CHCl_3$		THF		PhCN	
		abs. (nm)	emis. (nm)	abs. (nm)	emis. (nm)	abs. (nm)	emis. (nm)	abs. (nm)	emis. (nm)	abs. (nm)	emis. (nm)
model PF		385	413	387	415	389	416	393	417	396	421
model PDI		568	584	574	601	576	607	567	599	582	612
PF-PDI	**PF** emission	385	412	387	415	388	418	393	417	393	420
	PDI emission	568[b]	590	576[b]	602	582[b]	614	571[b]	600	587[b]	615

[a] $\lambda_{ex} = 375$ nm for **model PF** and **PF-PDI** and $\lambda_{ex} = 543$ nm for **model PDI** and **PF-PDI**. [b] Values taken from the excitation spectra due to the low concentration of the **PDI** units.

TABLE 2: Fluorescence Quantum Yield of Model PF, Model PDI, and PF-PDI in Toluene and THF[a]

			PF-PDI		
			PF excitation		**PDI** excitation
solvent	**model PF**	**model PDI**	**PF** emission	**PDI** emission	**PDI** emission
toluene	0.67	0.98	0.51	0.14	0.90
THF	0.60	0.97	0.44	0.02	0.15

[a] $\lambda_{ex} = 375$ nm for **model PF** and **PF-PDI** and $\lambda_{ex} = 543$ nm for **model PDI** and **PF-PDI**.

S_0-S_1 electronic transition ($\varepsilon = 42\,000$ M^{-1} cm^{-1}) oriented parallel to the long molecular axis.[31] Compared to toluene, the absorption maximum of the **model PDI** subunit shifts to slightly shorter (longer) wavelengths in THF (PhCN). This correlates with the polarizability of THF and PhCN as compared to toluene and suggests that either both the ground and the excited state have a negligible permanent dipole moment or that the change in dipole moment upon excitation is negligible. This system displays one emission band around 610 nm with a shoulder at 660 nm. No tendency toward aggregation in the concentration ranges used for the experiments was observed in the steady-state measurements of the **model PDI**.[32] In both solvents, the value of the fluorescence quantum yield is close to unity.

PF-PDI. The absorption spectra of **PF-PDI** approximately consist of the superposition of the corresponding spectra of the **model PF** and **model PDI** moieties. It shows an intense absorption band peaking at 390 nm attributed to the polyfluorene backbone and a very small absorbance in the 470−600 nm region due to the low ratio of the **PDI** units relative to the **PF** units (see Figure 2 inset).

The emission spectra of the **PF-PDI** were recorded by selective excitation of the **PF** or **PDI** moieties. Stokes shifts found for the **PDI** units are rather small in all solvents (850 cm^{-1}), while they reach higher values (around 1600 cm^{-1}) for **PF** moieties. Upon excitation of the **PDI** unit (543 nm), the **PF-PDI** emission recorded in toluene shows a characteristic similar to the **model PDI** compound except for a small bathochromic shift (100 cm^{-1}) of the emission maximum. The fluorescence quantum yield is 0.90 in toluene and drops to 0.15 in THF, indicating the presence of a substantial deactivation pathway of the local excited state (LES) of the **PDI** in a polar solvent. The influence of the solvent polarity suggests the opening up of a new decay channel. However, the emission still occurs from the LES of the **PDI**, as no significant or systematic shift is observed in the emission maxima.

In contrast, the excitation of the **PF** (375 nm) reveals fluorescence emission features attributed to both **PF** and **PDI** parts. The presence of the **PDI** emission at this excitation wavelength points to the occurrence of an intrachain excitation energy transfer from the **PF** to the incorporated **PDI** chromophore. The probability of occurrences of interchain interactions is low due to the small ratio of the **PDI** subunits and the low concentration of the polymer solution. A spectral overlap between the **PF** emission and **PDI** absorption is displayed in the Supporting Information (SI), Figure 1 SI. An overall quantum yield (emission from the **PF** and **PDI** parts) of 0.65 is measured in toluene with a value of 0.51 for the **PF** part and 0.14 for the **PDI** part. In toluene, the quantum yield values obtained for **PF-PDI** suggest that about 16% of the quanta absorbed by the **PF** part end up in the **PDI**.[45] Apparently, fluorescence and energy transfer are the main deactivating pathways of the LES of the **PF** units. In THF, the overall quantum yield decreases substantially (0.46) pointing to the occurrence of competitive excited-state processes that lead to a quenching of **PF** and **PDI** S_1 states.

Single-Molecule Wide-Field Imaging. Steady-state measurements indicate that 16% of the absorbed quanta end up in a **PDI** unit when the **PF** units are excited in the **PF-PDI** copolymer. However, because of the high polydispersity of the copolymer and the limited amount of **PDI** that are present, it is important to realize that not all copolymer chains might actually contain **PDI** units. Before proceeding with time-resolved experiments and discussing energy transfer efficiencies in more detail, it is crucial to determine this **PF polymer fraction**. For this, wide-field images and fluorescence intensity trajectories of individual polymer chains dispersed in a PMMA film were recorded. Two excitation laser were used, 375 and 532 nm, to selectively excite the **PF** and **PDI** units. First, an image was constructed by briefly exposing the sample to 375 nm excitation light for 5 s. This allowed us to visualize all the polymer chains (see Figure 3A for the integrated image of the 10 recorded frames). In the next step, a movie was recorded of the same area using 532 nm excitation until all molecules were photobleached (see Figure 3B for first frame). In this way, the **PDI**-containing copolymers can be identified, and fluorescence intensity time trajectories can also be constructed. After this, a 5 s long control movie was taken with 375 nm excitation to verify whether all the copolymers were still present and whether the **PF** units were still emitting (see Figure 3C for the integrated image of the 10 recorded frames). Comparing the spots that are present in Figure 3A,C versus the spots in Figure 3B indicates that there are eight spots (indicated with yellow squares) that do not have a corresponding spot in Figure 3B. The other six spots do have a corresponding spot in Figure 3B (indicated there with red squares). Control experiments were also performed, indicating that in pure PMMA no emissive spots were present when excited with 375 nm (data not shown), confirming that the spots are indeed from the **PF-PDI** copolymers. In total, 121 copolymer molecules were visualized with 375 nm excitation, of which 62% showed corresponding emission when excited with 532 nm and 38% did not (**PF polymer fraction**). Figure 3 also shows two fluorescence intensity trajectories of **PDI** containing **PF-PDI** copolymers indicated in Figure 3B. In example 1, two intensity levels can be seen, probably indicative of the presence of two **PDI** subunits

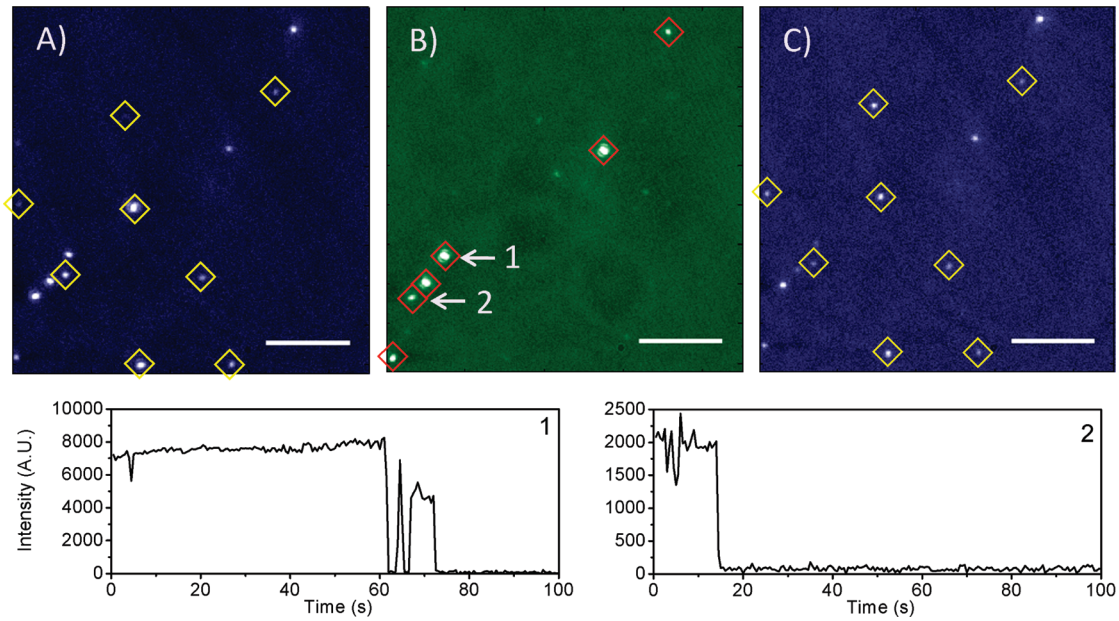

Figure 3. Wide-field images and fluorescence intensity trajectories of individual **PF-PDI** copolymers dispersed in a PMMA film. (A) Wide-field image recorded with 375 nm excitation light. The **PF** units are the absorbing moieties in this image, and fluorescence is emitted by either the **PF** or **PDI** units. The yellow squares indicate copolymers that do not display emission when excited with 532 nm (see Figure 3B). (B) Wide-field image recorded with 532 nm excitation light of the same area as Figure 3A. The **PDI** subunits are the absorbing and emitting moieties in this image. The red squares indicate copolymers that contain **PDI** subunits. The area was illuminated until all spots were photobleached. (C) Wide-field image recorded with 375 nm excitation light after bleaching of all the **PDI** subunits (see Figure 3B). The yellow squares again indicate copolymers that do not display emission when excited with 532 nm (see Figure 3B). Inset 1 represents an example of a **PF-PDI** copolymer containing 2 **PDI** chromophores. Inset 2 is a **PF-PDI** copolymer containing 1 **PDI** chromophore.

in this **PF-PDI** molecule. Photobleaching is observed after 72 s. Example 2 displays a single intensity level and single step photobleaching after 15 s, indicative of the presence of a single **PDI** subunit. The exact number of **PDI** units present[46] in each **PDI** containing **PF-PDI** molecules can be found in the SI. When discussing energy transfer efficiencies the presence of this **PF polymer fraction** will bias the data, lowering the actual energy transfer efficiency that occurs in **PDI**-containing **PF-PDI** copolymers. On the basis of the wide-field microscopy results (assuming that only 62% of the **PF-PDI** copolymer molecules actually contain **PDI** subunits), the energy transfer efficiency in the **PDI**-containing **PF-PDI** fraction is not 16%, as suggested by ensemble measurements, but rather 26%.

Time-Resolved Fluorescence Measurements. In order to obtain better insight into the excited-state properties of the investigated systems, a series of time-resolved fluorescence experiments were performed in toluene and THF. The fluorescence decay times of the **model PF**, **model PDI**, and **PF-PDI** obtained by TC-SPC experiments are given in Table 3. To help in identifying to which excited-state processes a decay component is related, a global analysis of the results obtained in the emission domain (from 450 until 700 nm) of the **PF-PDI** was performed. The fluorescence was recorded at 10 different wavelengths (see also Figure 4 SI and Figure 5 SI for the actual fluorescence decay curves) in the emission spectrum and the wavelength dependencies of the partial amplitudes are displayed in Figure 4.

Model PF. The **model PF** compound decays in toluene and THF biexponentially and can be best fitted with two time constants of 0.35 (86%) and 0.12 (14%) ns. A biexponential decay has been reported before in the literature for polyfluorene and it is not uncommon for conjugated polymers to exhibit multiexponential decay behavior due to the heterogeneity of their structure.[47,48]

Model PDI. The fluorescence kinetic properties of the **model PDI** system in toluene were investigated previously in our group.[49] Briefly, a biexponentially decay is found with time constants of 5.5 ns (94%) attributed the decay times of the LES and 0.48 ns (6%) attributed to a conformational relaxation process of the bay substituents.[49−52] As described in the literature, this amplitude changes from positive to negative contributions, crossing zero at 585 nm.[49] Since the fluorescence quantum yield approaches unity, the fluorescence rate constant, k_f, can be determined at the crossing point. A value of 1.85×10^8 s^{-1} was inferred for **model PDI** in toluene at 585 nm where the decay is monoexponential.

PF-PDI. As indicated by the stationary measurements, the photophysical properties of **PF-PDI** depend on the excitation wavelength (which unit is excited) and the solvent polarity. To investigate the kinetics and the excited states involved, **PF-PDI** was selectively excited with laser pulses of 543 and 375 nm wavelength.

TABLE 3: Fluorescence Decay Times and Their Partial Contributions of Model PF, Model PDI, and PF-PDI in Toluene and THF Measured by TC-SPC (λ_{ex} = 375 nm, λ_{ex} = 543 nm)

			PF-PDI	
solvent	**model PF** τ (ns)	**model PDI** τ (ns)	**PF** excitation τ (ns)[a]	**PDI** excitation τ (ns)
toluene	0.35 (86%)	5.5 (94%)[b]	0.14	
	0.12 (14%)	0.48 (6%)[b]	0.35	0.60 (2%)
			2.70	2.60 (7%)
			4.80	4.67 (91%)
THF	nd[c]	nd[c]	0.14	
			0.36	0.30 (22%)
			1.12	1.14 (56%)
			2.70	2.70 (17%)
			4.80	4.80 (4%)

[a] See Figure 4 for amplitudes. [b] Taken from ref 49. [c] nd = not determined.

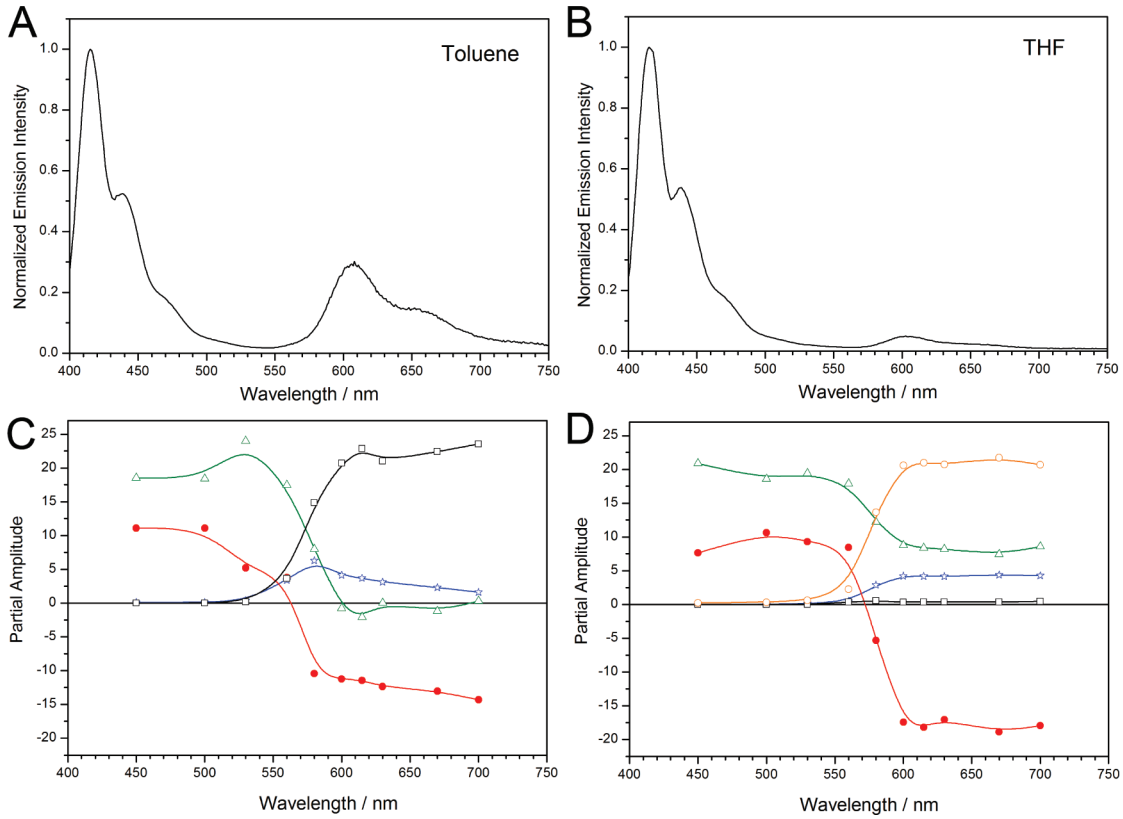

Figure 4. Normalized steady-state emission spectra of **PF-PDI** in toluene (A) and THF (B) ($\lambda_{ex} = 375$ nm). Wavelength dependence of the partial amplitudes of fluorescence decay times of **PF-PDI** obtained by TC-SPC experiments in toluene (C) [0.14 ns (●), 0.36 ns (Δ), 2.7 ns (*), 4.8 ns (□)] and THF (D) [0.14 ns (●), 0.36 ns (Δ), 1.12 ns (○), 2.7 ns (*), 4.8 ns (□)]; global $\chi^2_{toluene} = 1.04$, $\chi^2_{THF} = 1.008$.

PF-PDI, 543 nm Excitation. A triexponential decay is observed in toluene when the **PF-PDI** compound is excited at 543 nm (see Table 3). The long component with a major amplitude (91%) is attributed to the decay of the **PDI** units. This fluorescence decay time (4.67 ns) of the incorporated **PDI** chromophore in the polymer chain is shorter when compared to the corresponding **model PDI** system. The latter can, to a certain extent, be accounted for by the drop in the fluorescence quantum yield (from 0.98 to 0.9), which can be attributed to the opening-up of nonradiative decay channels, due to the attachment of the polymer chain to the **PDI** unit. Similar as for the **model PDI**, there is a small (2%) 0.6 ns component that can be attributed to a conformational relaxation process of the bay substituents. Besides this, a 2.6 ns component is also present (vide infra).

The excited-state processes in THF correspond only partially to the observed processes in toluene (see Table 3). The fluorescence traces were best fitted with four time constants. The long decay component of 4.8 ns now has a strongly reduced amplitude (4%). The presence of two additional short components of 0.30 ns (22%) and 1.14 ns (with a major amplitude of 56%) in a polar solvent, its absence in the **model PDI** fluorescence measurements, together with the decrease of the fluorescence quantum yield suggests the formation of a state with a charge transfer (CT) character (vide infra). The small component related to the conformational relaxation process of the bay substituents can not be extracted from the fit, probably due to the presence of the 0.3 and 1.14 ns component, which both have large amplitudes and most probably mask the 0.6 ns decay component. The 2.7 ns component can also be observed here (vide infra).

PF-PDI, 375 nm Excitation. The excitation of the **PF** moiety of the **PF-PDI** system (375 nm), revealed a rather complex kinetic behavior when the fluorescence is collected and analyzed in the 450−700 nm spectral region where both subunits emit. The traces were globally analyzed and could be best fitted with four and five time constants in toluene and THF, respectively (Table 3).

When exciting the **PF-PDI** system into the **PF** part, the photophysical behavior should be similar to that of the **model PF**. The fact that a low number of **PDI**s are incorporated in the copolymer made us anticipate that the emission occurring from the LES of **PF** with a time constant of 0.36 ns will not be significantly affected. However, a difference is already seen in the stationary measurements of **PF-PDI**. Fluorescence quantum yield measurements of **PF-PDI** and **model PF** in toluene and the wide-field imaging results (vide supra) suggest that in the **PDI**-containing **PF-PDI** fraction, 26% of the energy can be transferred to the **PDI** units, which emit with a fluorescence quantum yield of 0.9. This means that the inserted **PDI** chromophore can act as a trap for the excitation energy along the linear polymer chain of **PF-PDI**.

In toluene, a 0.35 ns component attributed to the fluorescence decay of the **PF** subunit is recovered with a positive amplitude in the 450−580 nm region (see Figure 4). Similarly, a decay component of 4.8 ns, which displays a positive amplitude in the **PDI** emission region can be attributed to the fluorescence of the **PDI** subunit. Two additional components of 0.14 and 2.7 ns were found. The 0.14 ns features a positive amplitude (decay component) in the emission region of the **PF** and a negative amplitude (rise component) in the emission region of the **PDI** subunit. This component clearly indicates a process in which electronic excitation energy of the **PF** moieties is most probably transferred to the neighboring **PDI** chromophores. The 2.7 ns component is similar in its amplitude-to-wavelength dependence to the 4.8 ns component (although smaller in

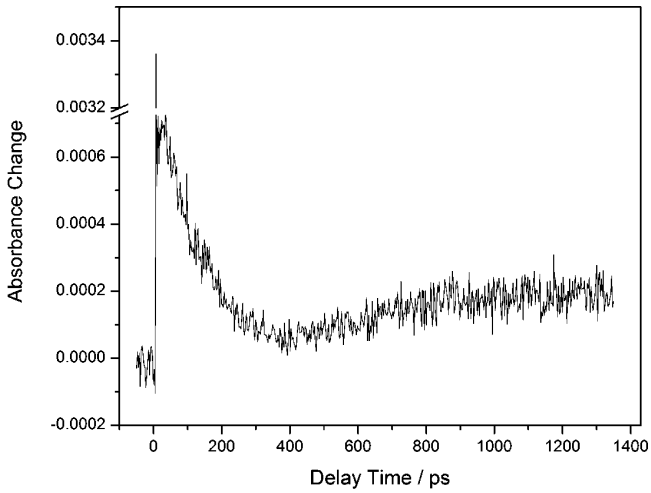

Figure 5. Femtosecond transient absorption decay trace of **PF-PDI** in THF; $\lambda_{excit} = 395$ nm, $\lambda_{detect} = 730$ nm.

amplitude), pointing to the presence of an additional emitting species in the **PDI** emission region. This component is only observed in the experiments with the copolymer and is independent of the solvent polarity (vide infra). The fact that in the copolymer in toluene no 0.12 ns component (second decay component of the **PF** unit with small amplitude) could be retrieved is probably due to the difficulty of the fit procedure to discriminate it from the 0.14 ns component (energy transfer component, which has a large amplitude).

A strongly reduced fluorescence observed in the polar solvent THF upon 375 nm excitation indicates that a CT might occur after indirect (via **PF**) excitation of the **PDI** subunit. The kinetic behavior of **PF-PDI** observed in the time-resolved experiments appears slightly more complex, involving five time constants. The four time constants found in toluene are also recovered in THF. The strongly reduced contribution of the 4.8 ns component as seen by the minute partial amplitude indicates that only a small fraction of the **PDI** units is unquenched. An extra component of 1.12 ns with a large and positive amplitude over the **PDI** emission region is found. Compared to the data in toluene, the 0.36 ns component has positive amplitudes in the **PF** and **PDI** emission regions (see Figure 4C,D). This component corresponds to a superposition of two decay constants of 0.35 ns related to the main **PF** fluorescence decay (large amplitude in the blue part of the spectrum) and an additional component with a value close to 0.35 and attributed to an extra decay of the **PDI** chromophore (positive amplitude in the red part of the spectrum, probably relating to CT formation).

To further investigate the nature of the quenching mechanism, ultrafast transient absorption experiments were performed. Femtosecond transient absorption experiments of **PF-PDI** in THF revealed a rising signal (increased absorption) on a nanosecond time scale at 730 nm (Figure 5). In toluene, no rise can be observed (see SI). Several studies reported in literature indicate that the species absorbing in this wavelength region corresponds to the radical anion of the **PDI** chromophore.[53,54] On the basis of the 543 nm excitation experiments, the stationary data and femtosecond experiments, this component can be attributed to a process leading to the formation of a state with CT character. In THF the energetic position of the CT state relative to the LES is lower with respect to toluene due to an energetic stabilization induced by the higher polarity of THF. This can lead to an increase of the change in free energy of charge separation to form a CT state. In solvents of higher polarity, like benzonitrile, the free energy change is expected to further increase, promoting the formation of the CT state even more. The decaying signal observed in the first part of this trace is related to a decrease in absorption of the excited state of the **PDI** subunit (S_1-S_n absorption), which partially overlaps with the **PDI** anion absorption band.[51] The intense peak close to 0 delay time is due to a fast scattering process induced by the pump beam on the probe transmission or to a coherent interaction of the two laser pulses.

To further elucidate the complex excited-state dynamics occurring in **PF-PDI**, an investigation of the possible excited-state dynamics is carried out. Three intramolecular competing processes are put forward: energy hopping along the polyfluorene polymer chain, energy transfer from **PF** to **PDI**, and electron transfer from the **PF** to the **PDI** units.

Excited-State Processes in PF-PDI. ***Energy Hopping.*** An energy transfer process that often occurs in polymer systems between similar chromophores and leads to a redistribution of the energy along the polymer chain is the so-called energy hopping process.[55−57] One requirement is that the emission spectrum of the chromophore (the **PF** in our case) must overlap to a certain extent with its own absorption spectrum. The overlap between the emission and absorption spectra of the **PF** unit is depicted in Figure 3 SI. In the conjugated polymer, the absorbing chromophore consists of several conjugated fluorene units, on which the energy is localized.[58] The kinetic analysis of the fluorescence decay recorded upon photoexcitation of the **PF** unit in toluene reveals four dynamical processes with distinct time constants (Table 3). The dynamics could initially involve an ultrafast energy hopping process (exciton hopping) which takes place along the polymer block prior to the energy transfer to the **PDI** unit.

Proofs of exciton hopping process were earlier reported in alternating polyfluorene copolymers with a distribution of hopping times in the 1−10 ps time range.[25] Exciton migration along the copolymer chain has been suggested to occur with an average hopping rate constant of $k_{hopp} = 10^{11}$ s^{-1} on isolated polyfluorene chains.[59] Assuming a conjugation length of 12 fluorene units on average, a total of eight conjugated segments separate two consecutive **PDI** chromophores (assuming a 100:1 **PF/PDI** ratio based on the reaction mixture ratio). This assumption leads roughly to a maximum total of four hopping steps (10−40 ps) for the singlet exciton to migrate from the excitation site (in the middle of the **PF** segment) to the **PDI** trap. As mentioned before, this is an average value, and a substantial fraction (38%, **PF polymer fraction**) of polymers do not even have **PDI** units.

Energy Transfer. Emission occurring from the **PDI** subunit is observed when exciting the **PF** subunit of the system, and a 0.14 ns time constant for energy transfer is found. This efficient intrachain excitation energy transfer to the **PDI** subunit takes place as a second step in the excited state. Fluorescence spectra, quantum yields, and picosecond time-resolved experiments of **PF-PDI** indicate that energy transfer is involved in the photophysics of this copolymer with 26% efficiency (vide supra). The **PDI** unit is then promoted into the S_1 state followed by a radiative deactivation of the LES with a time constant of 4.8 ns characteristic to the **PDI** moiety. A kinetic pathway is suggested in Scheme 1. It has to be noted that the 0.14 ns component is in fact a combination of two time constants corresponding to an energy transfer process (main amplitude) and the 0.12 ns (minute contribution) attributed to a second fluorescence decay of the **PF** subunits. The difficulty in distinguishing between the two components is thought to be

SCHEME 1: The Suggested Kinetic Pathway for PF-PDI in Toluene and THF upon Excitation of the PF Unit (375 nm)[a]

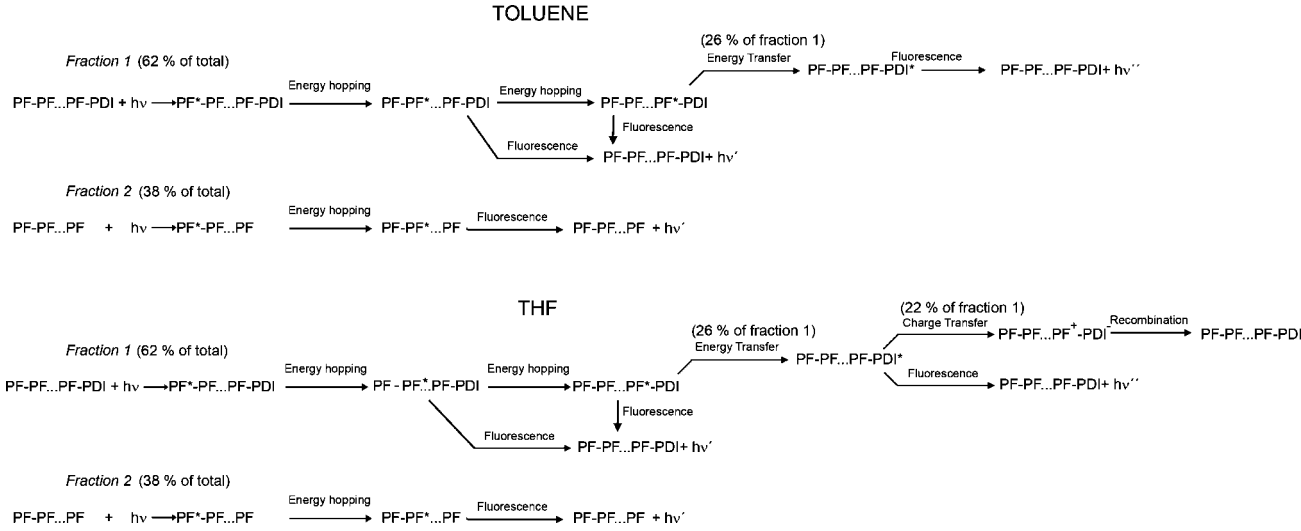

[a] The **PF-PDI** copolymer consists of two fractions: a large fraction that contains **PDI** units (fraction 1, 62% of total), and the **PF polymer fraction** (fraction 2, 38% of total).

due to the reduced precision of the fit analysis software in discriminating between two close values of time constants.[60] However, due to the large amplitude of the 0.14 ns component and its significant negative value in the **PDI** emission region, this can be largely attributed to the energy transfer process.

As experimentally proven above, the excitation energy transfer takes place from the **PF** S_1 state to the **PDI** S_0 state. If one assumes that this is a point-to-point transition dipole interaction, the excitation energy transfer can be described by the Förster resonance energy transfer (FRET) theory (see SI for details on the obtained overlap integrals and R_0 values calculated for the **PF-PDI** system).[61,62] Although it was shown that the Förster approach can break down when working with conjugated polymers,[63,64] the values (e.g., energy transfer efficiency, etc.) obtained for the **PF-PDI** system studied here when using the Förster approach are qualitatively in good agreement with the experimental observed data. There are numerous reasons why the Förster approach might not be applicable in a given conjugated polymer. For the system reported herein, we only got good agreement between theory and experiments taking into account the heterogeneous distribution of excitation energy donors and acceptors in the conjugated polymers chains. For example, wide-field measurements indeed showed here (vide supra) that the actual energy transfer efficiency is higher than that obtained from ensemble measurements due to the presence of a polymer fraction that does not contain **PDI** chromophores (**PF polymer fraction**). Furthermore, the spectral overlap between **PF** and **PDI** had to be assessed carefully. The spectral overlap between the **PF** emission (energy donor) and **PDI** absorption (energy acceptor) is illustrated in Figure 1 SI. An important point to consider is that the fluorescence of the **PF** overlaps to a large extent with the S_0-S_2 transition of the **PDI**. Since the efficiency of energy transfer also depends on the relative orientation of the transition dipole moment of the donor and the acceptor (κ^2), the contributions of S_0-S_1 and S_0-S_2 transitions are to be taken into account in order to evaluate the Förster distance, R_0. The S_0-S_1 transition dipole moments of the **PF** and **PDI** systems are oriented almost parallel to their long molecular axis, whereas the S_0-S_2 transition dipole moment of the **PDI** is oriented perpendicular to this axis.[65] Therefore, the absorption spectrum of the **PDI** was deconvoluted into a series of Gaussian shape spectra. A plot of the deconvolution is shown in Figure 2 SI. Values of 8.9×10^{-16} l mol^{-1} cm^3 and 1.58×10^{-15} l mol^{-1} cm^3 were obtained in toluene and THF, respectively, for the overlap integral considering the S_0-S_1 **PDI** absorption band. The overlap integrals with the S_0-S_2 band were found to be 3×10^{-14} l mol^{-1} cm^3 and 3.5×10^{-14} l mol^{-1}cm^3 in toluene and THF, respectively. R_0 can be estimated in terms of experimentally accessible spectroscopic data.[66−68] The calculation leads to Förster radii of $R_0 = 2.6$ nm ($R_0 = 2.9$ nm) in toluene (THF) for the energy transfer considering the **PDI** S_0-S_1 transition and $R_0 = 2.2$ nm ($R_0 = 2.3$ nm) for toluene (THF) for the **PDI** S_0-S_2 transition. Finally, potential competitive deactivation processes, e.g., electron transfer, have to be considered as well (vide infra).

Electron Transfer. It was shown that **PF-PDI** in THF exhibits excited-state processes and kinetic parameters that differ significantly from those in toluene or those of the reference systems **PF** and **PDI**. In THF, the excited **PDI** is strongly quenched, indicating the opening up of a new channel. Following the excitation of the **PF**, the kinetic involving this subunits appears analogous to the one indicated in toluene (see also Scheme 1). An energy hopping mechanism is expected to be initially involved followed by an energy transfer to the **PDI** (rate constant 7.1×10^9 s^{-1}) and promoting this subunit into the LES. The **PDI** chromophore was reported to possess a large electron accepting ability ($E_{red} = -0.43$ V vs SCE in DMF +0.1 M Bu_4NPF_6), while the **PF** unit can act as an electron-donating material.[49,69−71]

The dependence on the solvent polarity leads to a systematic decrease of the fluorescence, and the additional channel opened in the S_1 deactivation of **PDI** points to a photoinduced CT. The process occurs from the electron-rich **PF** subunits to the adjacent electron poor **PDI** subunit, leading to the formation of a nonemitting excited-state species with efficient nonradiative deactivation character. The additional components (0.3 and 1.12 ns) retrieved in the TC-SPC experiments in THF together with the rise observed in the femtosecond transient absorption measurements can be attributed to the absorption of the **PDI** radical anion (see Figure 5) and are likely related to a photoinduced CT process. As estimated above, the excitation energy located on the **PF** subunit is believed to be transported (energy hopping and transfer) toward the **PDI** and found to

occur with time constants faster than the CT formation. The formation of the nonemitting CT state occurs after the energy transfer from **PF** to **PDI**, having the S_1 of the **PDI** as a precursor state (time constants of 0.30 and 1.12 ns). Assuming an energy transfer efficiency of 26% for the **PF-PDI** (vide supra), this indicates that the efficiency of the **PF** exciton conversion to charges is about 22% (about 85% of the excited **PDI** units lead to CT formation based on the quantum yields in Table 2), a significant value if one considers that the acceptor concentration is on average 1% (based on the synthesis ratio). The suggested kinetic scheme is depicted in Scheme 1 and accounts for three consecutive processes involved in the **PF-PDI** dynamics: exciton hopping (<10 ps), energy transfer (140 ps), and charge transfer (0.3 and 1.12 ns). We emphasize that the model is fully consistent with the data obtained in the time-dependent fluorescent measurements.

An extra time component of 2.7 ns is retrieved from the data analysis with amplitude-to-wavelength dependence that is similar to that of the 4.8 ns component (see Figure 4). The nature of this process is seen as an extra decay channel opening up in the deactivation pathway of the **PDI** subunit which is not solvent polarity dependent and is observed only in the copolymer. We suggest that this component could be attributed to the decay of a fraction of **PDI**s with a different conformation of the chromophore in the polymer chain. For similar perylenediimide chromophores embedded in polymer films, single-molecule spectroscopy demonstrated that different conformations are present, resulting in fractions with different decay times (one fraction has a shorter decay with a value of 3 ns).[72] Similar conformational distributions were also observed for other chromophores where different conformations displayed different decay times and emission spectra.[73,74] Nevertheless, it is evident that this fraction participates in the exciton transfer as an energy acceptor (fluorescence decay component of the **PDI** subunit) but is not involved in the electron transfer. As a result, this fraction of **PDI** chromophores is responsible for a large part of the remaining emission in the **PDI** emission range of the **PF-PDI** copolymer in THF. Its contribution shows the same proportionality to the major amplitude in both solvents. In addition, this component shows an equal contribution in the 375 and 543 nm excitation experiments, while in the **PDI** model compound this is not observed.

Conclusions

Steady-state and time-resolved spectroscopy corroborated with femtosecond transient absorption experiments were employed to investigate the exciton dynamics occurring in a **PF-PDI** copolymer. Following the excitation of the **PF** unit, an ultrafast energy hopping has been suggested as the mechanism responsible for the exciton diffusion along the conjugated polymer chain. For the polymer fraction containing **PDI** units, about 26% of the excitation energy is then transferred to a **PDI** chromophore with a time constant of 140 ps. On the basis of the reaction mixture of 100 fluorene units to 1 **PDI**, this value further underpins the efficiency of the energy transfer process since the polymer chain only contains a low amount of **PDI** units. The latter value of 26% was obtained using a wide-field microscopy technique that could identify the fraction of polymers that did not contain **PDI** units and correct the biased average value of 16% obtained from ensemble measurements. Subsequently, the excited-state decay of the **PDI** subunit is dependent on the solvent polarity, which influences the available decay channels. The formation of a CT state, having the **PDI** subunit as a precursor state, is found to occur in THF on a nanosecond time scale which then decays nonradiatively to the ground state. About 85% of the excited **PDI** units lead to CT formation in THF. The detailed kinetics investigated in this study could lead to further optimization of this efficiency, suggesting that an alternating copolymer consisting of one **PDI** chromophore to every 24 or less fluorene units could lead to a almost complete quenching of the photoexcited **PF**s.

Acknowledgment. T.V. thanks the "Fonds Voor Wetenschappelijk Onderzoek" for a postdoctoral fellowship. Financial support of the "Fonds voor Wetenschappelijk Onderzoek FWO" (Grant G.0366.06), the K. U. Leuven Research Fund (GOA 2006/2, Center of Excellence CECAT, CREA2007), the Flemish government (Long term structural funding- Methusalem funding and Tournesol 2009 project T2009.05), and the Federal Science Policy of Belgium (IAP-VI/27) is gratefully acknowledged. This work, as part of the European Science Foundation EUROCORES Program SONS, was supported from funds by the FWO and the E.C. sixth Frame-work Program (ERAS-CT-2003-980409).

Supporting Information Available: Additional information related to the fraction of removed free PDI units, energy transfer, calculation of the spectral overlap, overlap integral, the Förster radius, TC-SPC experimental data, femtosecond transient absorption decay trace of PF-PDI in toluene, histogram of the number of PDI units in the PF-PDI copolymer. This material is available free of charge via the Internet at http://pubs.acs.org.

References and Notes

(1) Sirringhaus, H.; Tessler, N.; Friend, R. H. *Science* **1998**, *280*, 1741–1744.
(2) Spanggaard, H.; Krebs, F. C. *Sol. Energy Mater. Sol. Cells* **2004**, *83*, 125–146.
(3) Burn, P. L.; Holmes, A. B.; Kraft, A.; Bradley, D. D. C.; Brown, A. R.; Friend, R. H.; Gymer, R. W. *Nature* **1992**, *356*, 47–49.
(4) Webster, G. R.; Burn, P. L. *Synth. Met.* **2004**, *145*, 159–169.
(5) Barbara, P. F.; Gesquiere, A. J.; Park, S.-J.; Lee, Y. J. *Appl. Phys. Lett.* **1991**, *58*, 1982–1984.
(6) Barbara, P. F.; Doo, Y. K.; Grey, J. K. *Synth. Met.* **2006**, *156*, 336–45.
(7) Yu, Z. H.; Barbara, P. F. *J. Phys. Chem. B* **2004**, *108*, 11321–11326.
(8) Gesquiere, A. J.; Lee, Y. J.; Yu, J.; Barbara, P. F. *J. Phys. Chem. B* **2005**, *109*, 12366–12371.
(9) Yu, J.; Lammi, R.; Gesquiere, A. J.; Barbara, P. F. *J. Phys. Chem. B* **2005**, *109*, 10025–10034.
(10) Park, S. J.; Gesquiere, A. J.; Yu, J.; Barbara, P. F. *J. Am. Chem. Soc.* **2004**, *126*, 4116–4117.
(11) Wöll, D.; Braeken, E.; Deres, A.; De Schryver, F. C.; Uji-i, H.; Hofkens, J. *Chem. Soc. Rev.* **2009**, *38*, 313–328.
(12) Ferreira, M; Olivati, C. A.; Machado, A. M.; Assaka, A. M.; Giacometti, J. A.; Akcelrud, L.; Oliveira, O. N. *J. Polym. Res.* **2007**, *14*, 39–44.
(13) Lupton, J. M.; Klein, J. *Synth. Met.* **2003**, *138*, 233–236.
(14) Lupton, J. M.; Craig, M. R.; Meijer, E. W. *Appl. Phys. Lett.* **2002**, *80*, 4489.
(15) Gomez, R.; Veldman, D.; Blanco, R.; Seoane, C.; Segura, J. L.; Janssen, R. A. J. *Macromolecules* **2007**, *40*, 2760–2772.
(16) Ego, C.; Marsitzky, D.; Becker, S.; Zhang, J. Y.; Grimsdale, A. C.; Mullen, K.; MacKenzie, J. D.; Silva, C.; Friend, R. H. *J. Am. Chem. Soc.* **2003**, *125*, 437.
(17) Li, A. Y.; Ziegler, A.; et al. *Chem.—Eur. J.* **2005**, *11*, 4450–4457.
(18) Sariciftci, N. S.; Smilowitz, L.; Heeger, A. J.; Wudl, F. *Science* **1992**, *258*, 1474.
(19) Janssen, R. A. J.; Hummelen, J. C.; Sariciftci, N. S. *MRS Bull.* **2005**, *30*, 33.
(20) Brabec, C. *Sol. Energy Mater. Sol. Cells* **2004**, *83*, 273.
(21) Yu, G.; Gao, J.; Hummelen, J. C.; Wudl, F.; Heeger, A. J. *Science* **1995**, *270*, 1789.
(22) Russell, D. M.; Arias, A. C.; Friend, R. H.; Silva, C.; Ego, C.; Grimsdale, A. C.; Müllen, K. *Appl. Phys. Lett.* **2002**, *80*, 2204–2206.
(23) Simas, E. R.; Gehlen, M. H.; Glogauer, A.; Akcelrud, L. *J. Phys. Chem. A* **2008**, *112*, 5054–5059.

(24) Inganas, O; Svensson, M; Zhang, F; Gadisa, A; Persson, N. K.; Wang, X; Andersson, M. R. *Appl. Phys. A: Mater. Sci. Process.* **2004**, *79*, 31–35.
(25) Jespersen, K. G.; Yartsev, A.; Pascher, T.; Sundström, V. *Synth. Met.* **2005**, *155*, 262–265.
(26) De, S.; Kesti, T.; Maiti, M.; Zhang, F.; Inganäs, O.; Yartsev, A.; Pascher, T.; Sundström, V. *Chem. Phys.* **2008**, *350*, 14–22.
(27) Da Como, E.; Scheler, E.; Strohriegl, P.; Lupton, J. M.; Feldmann, *J. Appl. Phys. A* **2009**, *95*, 61–66.
(28) Lupton, J. M.; Schouwink, P.; Keivanidis, P. E.; Grimsdale, A. C.; Müllen, K. *Adv. Funct. Mater.* **2003**, *13*, 154–158.
(29) Hattori, A.; Habuchi, S.; Vacha, M. *Chem. Lett.* **2009**, *38*, 234–235.
(30) Lide D. R. *Handbook of Physics and Chemistry*, 73rd ed.; CRC Press, Boca Raton, FL, 1992.
(31) Du, H.; Fuh, R. A.; Li, J.; Corkan, A.; Lindsey, J. S. *Photochem. Photobiol.* **1998**, *68*, 141.
(32) Geerts, Y., Müllen, K., Rettig, W., Strehmel, B., Schrader, S., Eds. *Applied Fluorescence in Chemistry, Biology, and Medicine*; Springer Verlag: Berlin, 1998; p 299.
(33) Vosch, T.; Fron, E.; Hotta, J.-I.; Deres, A.; Uji-i, H.; Idrissi, A.; Yang, J.; Dongho, K.; Puhl, L.; Haeuseler, A.; Müllen, K.; De Schryver, F. C.; Sliwa, M.; Hofkens, J. *J. Phys. Chem. C* **2009**, *113*, 11773–11782.
(34) Maus, M.; Rousseau, E.; Cotlet, M.; Schweitzer, G.; Hofkens, J.; Van der Auweraer, M.; De Schryver, F. C. *Rev. Sci. Instrum.* **2001**, *72*, 36–40.
(35) Program developed in a cooperation between the Management of Technology Institute (Belarusian State University) and The Division of Photochemistry and Spectroscopy (University of Leuven).
(36) Boens, N.; Qin, W. W.; Basaric, N.; Hofkens, J.; Ameloot, M.; Pouget, J.; Lefevre, J. P.; Valeur, B.; Gratton, E.; Vandeven, M.; Silva, N. D.; Engelborghs, Y.; Willaert, K.; Sillen, A.; Rumbles, G.; Phillips, D.; Visser, A.; van Hoek, A.; Lakowicz, J. R.; Malak, H.; Gryczynski, I.; Szabo, A. G.; Krajcarski, D. T.; Tamai, N.; Miura, A. *Anal. Chem.* **2007**, *79*, 2137–2149.
(37) O'Connor, D. V.; Philips, D. *Time-Correlated Single Photon Counting*; Academic Press: London, 1984.
(38) Schweitzer, G.; Xu, L.; Craig, B.; De Schryver, F. C. *Opt. Commun.* **1997**, *142*, 283–288.
(39) Klaerner, G.; Miller, R. D. *Macromolecules* **1998**, *31*, 2007.
(40) Muls, B.; Uji-i, H.; Melnikov, S.; Moussa, A.; Verheijen, W.; Soumillion, J. P.; Josemon, J.; Mullen, K.; Hofkens, J. *ChemPhysChem* **2005**, *6*, 2286–2294.
(41) Jo, J. H.; Chi, C. Y.; et al. *Chem.—Eur. J.* **2004**, *10*, 2681–2688.
(42) Teetsov, J.; Fox, M. A. *J. Mater. Chem.* **1999**, *9*, 2117.
(43) Hosoi, K.; Mori, T.; Mizutani, T.; Yamamoto, T.; Kitamura, N. *Thin Solid Films* **2003**, *438*, 201.
(44) Kulkarni, A. P.; Kong, X. X.; Jenekhe, S. A. *J. Phys. Chem. B* **2004**, *108*, 8689.
(45) This 16% comes from the fluorescence quantum yield of 0.14 observed for the PDI units when exciting the PF units in toluene divided by 0.9 (the fluorescence quantum yield of PDI in PF-PDI).
(46) Dedecker, P.; Muls, B.; Deres, A.; Uji-i, H.; Hotta, J.; Sliwa, M.; Soumillion, J. P.; Mullen, K.; Enderlein, J.; Hofkens, J. *Adv. Mater.* **2009**, *21*, 1079–1090.
(47) Byun, H. Y.; Chung, I. J.; Shim, H-K; Kim, C. Y. *Chem. Phys. Lett.* **2004**, *393*, 197–203.
(48) Dias, F. B.; Knaapila, M.; Monkman, A. P.; Burrows, H. D. *Macromolecules* **2006**, *39*, 1598–1606.
(49) Fron, E.; Schweitzer, G.; Osswald, P.; Würthner, F.; Marsal, P.; Beljonne, D.; Müllen, K.; De Schryver, F. C.; Van der Auweraer, M. *Photochem. Photobiol. Sci.* **2008**, *7*, 1509–1521.
(50) Flors, C.; Oesterling, I.; Schnitzler, T.; Fron, E.; Schweitzer, G.; Sliwa, M.; Herrmann, A.; van der Auweraer, M.; De Schryver, F. C.; Mullen, K.; Hofkens, J. *J. Phys. Chem. C* **2007**, *111*, 4861.
(51) Fron, E.; Pilot, R.; Schweitzer, G.; Qu, J.; Herrmann, A.; Müllen, K.; Hofkens, J.; Van der Auweraer, M.; De Schryver, F. C. *Photochem. Photobiol. Sci.* **2008**, *7*, 597–604.
(52) Osswald, P.; Wurthner, F. *J. Am. Chem. Soc.* **2007**, *129*, 14319–14326.
(53) Gosztola, D.; Niemczyk, M. P.; Svec, W. A.; Lukas, A. S.; Wasielewski, M. R. *J. Phys. Chem. A* **2000**, *104*, 6545–6551.
(54) Kircher, T.; Löhmannsröben, H.-G. *Phys. Chem. Chem. Phys.* **1999**, *1*, 3987–3992.
(55) Herz, L. M.; Silva, C.; Grimsdale, A. C.; Müllen, K.; Phillips, R. T. *Phys. Rev. B* **2004**, *70*, 165207.
(56) Barbara, P. F.; Gesquiere, A. J.; Park, S. J.; Lee, Y. J. *Acc. Chem. Res.* **2005**, *38*, 602–610.
(57) Lin, H. Z.; Tabaei, S. R.; Thomsson, D.; Mirzov, O.; Larsson, P. O.; Scheblykin, I. G. *J. Am. Chem. Soc.* **2008**, *130*, 7042–7051.
(58) Lammi, R. K.; Barbara, P. F. *Photochem. Photobiol. Sci.* **2005**, *4*, 95–99.
(59) Fernando, B. D.; Manisankar, M.; Susanne, I. H.; Andrew, P. M. *J. Chem. Phys.* **2005**, *122*, 054904.
(60) Eaton, D. F. *Pure Appl. Chem.* **1990**, *62*, 1631–1648.
(61) Förster, Th. *Z. Naturforsch. A* **1949**, *4*, 321–327.
(62) Förster, Th. *Radiat. Res. Suppl.* **1960**, *2*, 326–339.
(63) Wong, K. F.; Bagchi, B.; Rossky, P. J. *J. Phys. Chem. A* **2004**, *108*, 5752–5763.
(64) Wiesenhofer, H.; Beljonne, D.; Scholes, G. D.; Hennebicq, E.; Brédas, J. L.; Zojer, E. *Adv. Funct. Mat.* **2005**, *15*, 155–160.
(65) Belfield, K. D.; Bondar, M. V.; Kachkovsky, O. D.; Przhonska, O. V.; Yao, S. *J. Lumin.* **2007**, *126*, 14.
(66) Van Der Meer, B. W.; Coker, G. III; Simon, Chen S.-Y. *Resonance Energy Transfer: Theory and Data*; Wiley-VCH: New York, 1994.
(67) Maus, M.; De, R.; Lor, M.; Weil, T.; Mitra, S.; Wiesler, U.-M.; Herrmann, A.; Hofkens, J.; Vosch, T.; Müllen, K.; De Schryver, F. C. *J. Am. Chem. Soc.* **2001**, *123*, 7668–7676.
(68) Fron, E.; Bell, T. D. M.; Van Vooren, A.; Schweitzer, G.; Cornil, J.; Beljonne, D.; Toele, P.; Jacob, J.; Müllen, K.; Hofkens, J.; Van der Auweraer, M.; De Schryver, F. C. *J. Am. Chem. Soc.* **2007**, *129*, 610–619.
(69) Sisk, W. N.; Kang, K.-S.; Raja, M. Y. A.; Farahi, F. *Int. J. Optoelectron.* **1995**, *10*, 95–103.
(70) Kanibolotsky, A. L.; Berridge, R.; Skabara, P. J.; Perepichka, I. F.; Bradley, D. D. C.; Koeberg, M. *J. Am. Chem. Soc.* **2004**, *126*, 13695–13702.
(71) Goldsmith, R. H.; Sinks, L. E.; Kelley, R. F.; Betzen, L. J.; Liu, W. H.; Weiss, E. A.; Ratner, M. A.; Wasielewski, M. R. *Proc. Natl. Acad. Sci. U.S.A.* **2005**, *102*, 3540.
(72) Hofkens, J.; Vosch, T.; Maus, M.; Kohn, F.; Cotlet, M.; Weil, T.; Herrmann, A.; Müllen, K.; De Schryver, F. C. *Chem. Phys. Lett.* **2001**, *333*, 255.
(73) Stracke, F.; Blum, C.; Becker, S.; Mullen, K.; Meixner, A. J. *ChemPhysChem* **2005**, *6*, 1242–1246.
(74) Braeken, E.; Marsal, P.; Vandendriessche, A.; Smet, M.; Dehaen, W.; Vallee, R. A. L.; Beljonne, D.; Van der Auweraer, M. *Chem. Phys. Lett.* **2009**, *472*, 48–54.

JP909295H